J. Meas. Sci. Instrum., 2024, 15(1): 72-82.
DOI: 10.62756/jmsi.1674-8042.2024008

http://jmsi.publish.founderss.cn/
jmsi@nuc.edu.cn

Sliding mode control of excavator electro-hydraulic system based on linear extended state observer

ZHANG Sen, ZHANG Ping*, ZHAO Zhe

School of Mechanical and Electrical Engineering, Xi'an University of Architecture and Technology, Xi'an 710055, China

***Corresponding author:** ZHANG Ping (zp_80@163.com)

Received: October 9, 2023 **Revised:** December 28, 2023 **Accepted:** January 18, 2024

Abstract: The actual working environment of unmanned excavation robot is harsh. In order to improve the trajectory tracking accuracy of bucket under load disturbance, a nonlinear mathematical model of electro-hydraulic system of digging robot was established, and a sliding mode controller (SMC) based on linear extended state observer (LESO), called SMC-LESO, was designed. Based on the displacement signal of the piston rod of the bucket cylinder, the velocity, the acceleration, the load disturbance and uncertain factors of the system were estimated by the LESO. On this basis, SMC-LESO was completed, and the Lyapunov stability of the controller was proved. The co-simulation model of electro-hydraulic proportional control system of the excavator was established. Compared with proportional-integral-derivative (PID) controller and SMC, the simulation results show that the designed controller can effectively suppress the disturbance, and has high displacement tracking accuracy and robustness.

Key words: unmanned excavation robot; electro-hydraulic system; linear extended state observer (LESO); sliding mode controller (SMC); displacement tracking control

0 Introduction

In order to adapt to the dangerous and harsh working environment, as well as to cope with increasing operational accuracy and efficiency requirements, excavators are required to improve their unmanned and intelligent control level continuously. The unmanned excavation robot is the product of deep integration of traditional excavator with artificial intelligence, automatic control, wireless communication and other technologies[1,2]. When the excavator is working, the digging load is unpredictable. However, as an important part of trajectory tracking control, the control of electro-hydraulic system of excavator robot has many nonlinear factors. Since there is no human participation in the unmanned excavation process, to reduce the influence of these factors on the trajectory tracking of the working device of the unmanned excavation robot, the control system needs better control performance[3].

Proportional-integral-derivative (PID) controllers have been used in automatic control systems of excavation robots owing to their structural simplicity and better stability, and thus the trajectory tracking accuracy is improved[4]. However, PID parameter tuning is a troublesome and time-consuming task. At present, fuzzy algorithm[5], particle swarm optimization[6], genetic algorithm[7] and ant colony algorithm[8] have been used to optimize the parameters of PID controller. Due to the complexity of the electro-hydraulic system of excavator robot, the nonlinearity of the system, the uncertainty of the external load and other factors, PID controller is unable to meet the requirements of trajectory control accuracy. Li et al.[9] proposed a new controller, which combines fuzzy-PI control and soft switch control, aiming to overcome the nonlinear and other uncertain factors in the electro-hydraulic control system of excavators, but the simulation model is linear. Hassan et al.[10] established a more accurate nonlinear model of the electro-hydraulic system of excavator robot, and put forward the interval Type-2 fuzzy controller, which can compensate the influence of nonlinear friction in the electro-hydraulic system of excavator robot and improve the position tracking accuracy of each actuator. However, it is difficult to deal with the fuzzy set of the controller. In the problem of excavating robot trajectory control, although the control effect of neural network-based control methods has been greatly improved compared with that of PID controllers, but the parameter selection of neural networks requires a large amount of theoretical and experimental data, and the practical application is more difficult[11,12].

Sliding mode controller(SMC) has good robustness to system uncertainty and external disturbance, and does not require an accurate mathematical model, so it is widely used in the control of electro-hydraulic systems[13]. Xu et al.[14] designed an SMC, which accurately tracks the expected trajectory of the electro-hydraulic position control system of the excavation robot and realizes hierarchical operation. Xu et al.[15] applied SMC to the impedance control of electro-hydraulic system so as to ensure that the controller has good control effect when the nonlinear system uncertainty exists. Liu et al.[16] proposed an SMC with variable switching coefficient, which can guarantee the robustness to system uncertainty. Aiming at the nonlinear characteristics and parameter disturbance and external disturbance of the electro-hydraulic position servo system, Wang et al.[17] applied the adaptive sliding mode control(ASMC) to the electro-hydraulic position servo control system, which effectively solves the chattering problem existing in the SMC and improves the tracking accuracy. Bai et al.[18] proposed an adaptive fuzzy sliding mode control (AFSMC) for the electro-hydraulic position control system, which can realize online adjustment of parameters and high-precision tracking. To solve the uncertainty and interference problems of valve-controlled asymmetric cylinder hydraulic system, Zhu et al.[19] proposed a robust feedback linearization control strategy combining sliding mode variable structure control and feedback linearization control.

Although the above nonlinear control methods are effective, more sensors are required to achieve a better trajectory tracking effect, which increases the control cost. The introduction of the observer into the controller provides a new solution to this problem. Li et al.[20] proposed an adaptive neural network terminal sliding mode control (ANTC), which uses a higher-order sliding mode observer instead of system model parameters to estimate the unmeasurable or difficult-to-measure state variables of the system, effectively improving the transient response speed and steady-state control accuracy of the system. Yao et al.[21] proposed a model-free adaptive control method based on radial basis function(RBF) neural network disturbance observer, which solves the problems of parameter uncertainty and unknown load disturbance in the electro-hydraulic servo system of the water well drilling rig under propulsion conditions. The controller design of the device is more complicated.

Active disturbance rejection control (ADRC) results from PID based on classical control theory and modern control theory[22, 23]. As a new type of nonlinear robust control technology, it does not depend on the accurate mathematical model of controlled object. The extended state observer (ESO) is the central part of the ADRC, which can suppress disturbances by treating all uncertainties acting on the controlled object as unknown disturbances, expanding them into new state variables, and using the input and output information of the object to estimate and compensate them. The electro-hydraulic system inevitably faces load disturbance, difficulty in establishing accurate mathematical model, parameter uncertainty, nonlinearity and other factors, which can be dealt with by ADRC based on the concept of total disturbance with certain advantages[25,26]. To address the problem that ESO parameters are numerous and difficult to be adjusted, Gao et al.[27] proposed a linear active disturbance rejection control (LADRC) based on bandwidth method, in which the parameter determination of linear extended state observer (LESO) is more convenient. Huang et al.[28] prposed a sliding mode controller based on linear expansion state observer (SMC-LESO), which mainly discusses the performance of the controller under the premise of the influence of load changes on the natural frequency of the electro-hydraulic system, but the established model is a linear model.

For the unmanned excavation robot, the nonlinearity of its electro-hydraulic system and the uncertainty of load have a serious impact on the precise trajectory control of working device. In our work, we first established a nonlinear model of the electro-hydraulic system of the excavator robot. An LESO was selected to observe the nonlinear factors and load disturbance of the system, and then it was merged into the SMC to establish a sliding mode controller based on the linear extended observer (SMC-LESO), which was used as the controller of the electro-hydraulic system of the excavator robot. The controller can not only reduce the number of sensors used, but also does not need an accurate mathematical model of the controlled object. It has great advantages in practical engineering.

1 System model

1.1 Equipment description

Since the control principles of all oil cylinders of excavator robot are similar, the electro-hydraulic proportional position control system of bucket oil cylinder is selected for analysis. The basic control circuit of the bucket cylinder is shown in Fig.1, which mainly includes an electronic control system, a pilot valve, a main valve and an asymmetric hydraulic cylinder. The designed controller only needs the displacement of the hydraulic cylinder as the input, which can be measured by the displacement sensor installed on the hydraulic cylinder. The amplifier of electronic control system converts voltage signal into current signal, and then the current signal is transmitted to the pilot proportional pressure reducing valve. The pilot proportional pressure reducing valve generates the corresponding pilot pressure according to the control signal, and the main valve generates the corresponding displacement according to the magnitude of pilot pressure. The piston of the hydraulic cylinder is determined by the movement of the main valve spool and it is retracted or extended correspondingly.

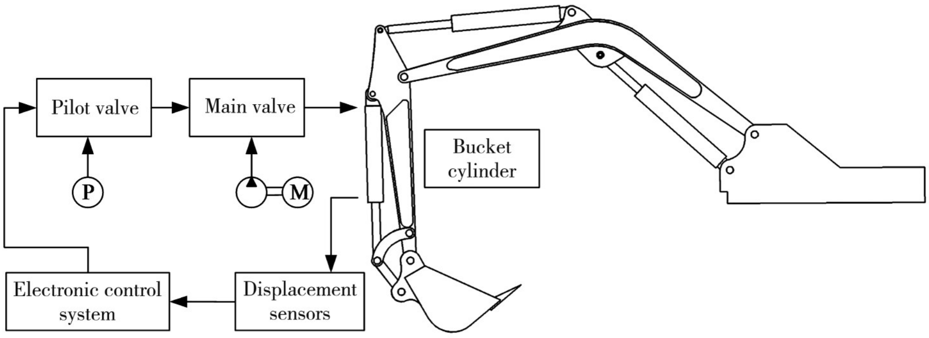

Fig. 1 Schematic diagram of control circuit of bucket cylinder

1.2 Mathematical model of electro-hydraulic position control system

The electro-hydraulic proportional position control system of bucket cylinder mainly includes controller, amplifier, electro-hydraulic proportional control and valve-controlled asymmetric cylinder. The control block diagram is shown in Fig.2. Based on this, the state space equation of the electro-hydraulic position control system of the bucket cylinder can be established, where u is the control voltage from the computer, i is the output current of amplifier, and p_{p} is the pilot pressure.

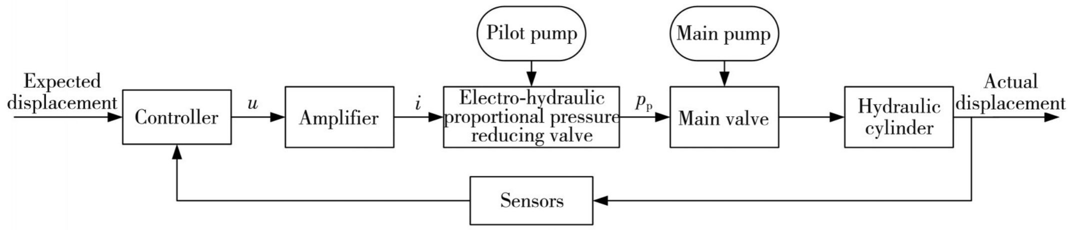

Fig. 2 Block diagram of electro-hydraulic proportional control system

1.2.1 Amplifier

The amplifier converts the output voltage signal of the controller into the current signal of the electro-hydraulic proportional pressure reducing valve. This process can be treated as a proportional level, and the mathematical model is defined as

$$i=k_{\mathrm{a}}u, \tag{1}$$

where i is the output current of amplifier, u is the control voltage from the computer, and k_{a} is the amplification coefficient of the amplifier.

1.2.2 Electro-hydraulic proportional control

It can be seen from Figs.1 and 2 that the proportional pressure reducing valve is driven to produce the corresponding pilot pressure by current i. Then the spool of multi-way valve is driven to produce the corresponding opening sizes by the pilot pressure. Generally, the response frequency of electro-hydraulic proportional valve is much greater than the response frequency of the system, so it can be simplified as a linear gain model. The first-order linear differential equation is expressed as

$$\tau_{\mathrm{v}}\dot{x}_{\mathrm{v}}+x_{\mathrm{v}}=k_{\mathrm{b}}i, \tag{2}$$

where x_{v} is the spool displacement of the main valve, and k_{b} is the amplification coefficient.

The above model can be further simplified as

$$x_{\mathrm{v}}=k_1 u, \tag{3}$$

where k_1 is the gain of electro-hydraulic proportional valve.

1.3 Mathematical model of valve-controlled asymmetric hydraulic cylinder

1.3.1 Force balance equation of hydraulic cylinder

The force balance equation of bucket hydraulic cylinder is expressed as

$$p_1A_1-p_2A_2=M\ddot{x}_{\mathrm{p}}+B_{\mathrm{c}}\dot{x}_{\mathrm{p}}+Kx_{\mathrm{p}}+F_{\mathrm{L}}, \tag{4}$$

where p_1 is the pressure of rodless chamber; p_2 is the pressure of rod chamber; A_1 and A_2 are the effective working areas facing of rodless and rod chambers, respectively; x_p is the displacement of the piston rod; M is the total equivalent mass of piston rod and load; B_c is the viscous damping coefficient of piston rod and load; K is the equivalent spring stiffness of the load, which is simplified to 0; and F_L is the external load force, assuming that it is at least first derivative.

1.3.2 Flow continuity equation of hydraulic cylinder

The flow continuity equation of the bucket hydraulic cylinder is calculated by

$$\begin{cases} Q_1 = A_1\dot{x}_p + C_i(p_1 - p_2) + C_o p_1 + \dfrac{V_1}{\beta_e}\dot{p}_1, \\ Q_2 = A_2\dot{x}_p - C_i(p_1 - p_2) - C_o p_2 - \dfrac{V_2}{\beta_e}\dot{p}_2, \end{cases} \tag{5}$$

where Q_1 is the flow in rodless chamber; Q_2 is the flow in rod chamber; C_i is the internal leakage coefficient, which takes 0 when ignoring the internal leakage; C_o is the outside leakage coefficient, which takes 0 when ignoring the outside leakage; β_e is the effective bulk modulus; $V_1 = V_{10} + A_1 x_p$ is the rodless chamber volume; $V_2 = V_{20} - A_2 x_p$ is the rod chamber volume; and V_{10} and V_{20} are the initial volumes of each rodless and rod cavity, respectively.

1.3.3 Dynamic flow characteristic equation of valve

To simplify the analysis, the following assumptions are put forward: the valve structure is symmetrical, the oil source pressure is constant, the return oil pressure is zero, each port of the main valve has the same flow coefficient, and the throttle orifice is symmetrical. The flow equations of the valve are expressed as

$$Q_1 = \begin{cases} C_d\omega x_v\sqrt{\dfrac{2}{\rho}(p_s - p_1)}, & x_v \geqslant 0, \\ C_d\omega x_v\sqrt{\dfrac{2}{\rho}(p_1 - p_r)}, & x_v < 0, \end{cases} \tag{6}$$

$$Q_2 = \begin{cases} C_d\omega x_v\sqrt{\dfrac{2}{\rho}(p_2 - p_r)}, & x_v \geqslant 0, \\ C_d\omega x_v\sqrt{\dfrac{2}{\rho}(p_s - p_2)}, & x_v < 0, \end{cases} \tag{7}$$

where C_d is the flow modification coefficient; ω is the valve area gradient; ρ is the oil density; p_s is the oil source pressure; and p_r is the oil return pressure, taking 0.

If the state variables are defined as $\boldsymbol{x} = [x_1 x_2 x_3]^T = [x_p \dot{x}_p \ddot{x}_p]^T$, the state equation of the system can be obtained according to Eqs. (1) − (7) as

$$\begin{cases} \dot{x}_1 = x_2, \\ \dot{x}_2 = x_3, \\ \dot{x}_3 = a_1 x_2 + a_2 x_3 + g(x_v)u + d, \\ y = x_1, \end{cases} \tag{8}$$

where

$$a_1 = -\frac{1}{M}\left(\frac{A_1^2}{V_1}\beta_e + \frac{A_2^2}{V_2}\beta_e\right),\ a_2 = -\frac{B_c}{M},$$

$$d = -\frac{\dot{F}_L}{M}, g(x_v) = \frac{C_d\omega K_1\beta_e}{M}\sqrt{\frac{2}{\rho}}\left(\frac{A_1}{V_1}g_1 + \frac{A_2}{V_2}g_2\right), g_1$$

$$= \mathrm{sgn}(u)\sqrt{p_s - p_1} + \mathrm{sgn}(u)\sqrt{p_1 - p_r},$$

$$g_2 = \mathrm{sgn}(u)\sqrt{p_2 - p_r} + \mathrm{sgn}(u)\sqrt{p_s - p_2},$$

$$\mathrm{sgn}(u) = \begin{cases} 1, & u \geqslant 0, \\ 0, & u < 0. \end{cases}$$

2 Controller design of electro-hydraulic proportional position control system for excavator

To reduce the number of sensors used, only the displacement sensor is used to obtain the displacement of the piston rod. The ESO is used to observe other state variables, load disturbance and other uncertain factors. These variables are expanded into new state variables as inputs of the controller. The block diagram of the controller is shown in Fig.3.

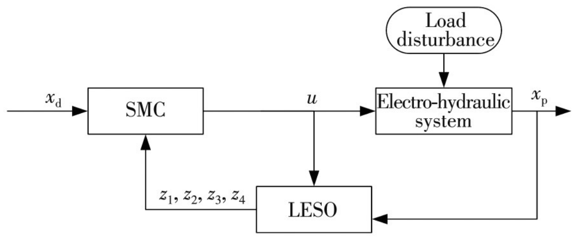

Fig. 3 Structure diagram of controller

2.1 Design of LESO

By defining the state variable $x = [x_1 x_2 x_3 x_4]^T = [x_p \dot{x}_p \ddot{x}_p D]^T$, Eq. (8) can be transformed into

$$\begin{cases} \dot{x}_1 = x_2, \\ \dot{x}_2 = x_3, \\ \dot{x}_3 = a_1 x_2 + a_2 x_3 + fu + x_4, \\ \dot{x}_4 = \dot{D}, \end{cases} \tag{9}$$

where f is the estimated value of $g(x_v)$, and $D = \Delta a_1 x_2 + \Delta a_2 x_3 + \Delta g(x_v)u + d$ is the comprehensive uncertainty of the system, which is derivable in the first order.

The variables $z_i (i = 1,2,3,4)$ are defined as the estimations of $x_i (i = 1,2,3,4)$ by the LESO, which are constructed as

$$\begin{cases} e = z_1 - y, \\ \dot{z}_1 = z_2 - \beta_1 e, \\ \dot{z}_2 = z_3 - \beta_2 e, \\ \dot{z}_3 = a_1 z_2 + a_2 z_3 + fu + z_4 - \beta_3 e, \\ \dot{z}_4 = -\beta_4 e, \end{cases} \tag{10}$$

where $\beta_i (i = 1,2,3,4)$ are the control gain of the LESO, Gao[27] gave a method to determine the gain of LESO by based on the concept of bandwidth, which is calculated as

$$\lambda(s)=s^4+\beta_1 s^3+\beta_2 s^2+\beta_3 s+\beta_4=(s+\omega_0)^4, \tag{11}$$

where ω_0 is the observer bandwidth. Then the control gain of LESO can be expressed as

$$\begin{cases}\beta_1=4\omega_0,\\ \beta_2=6\omega_0^2,\\ \beta_3=4\omega_0^3,\\ \beta_4=\omega_0^4.\end{cases} \tag{12}$$

2.2 Design of SMC

According to SMC theory, the sliding mode surface is defined as

$$\begin{cases}s=c_1 e_1+c_2 e_2+e_3,\\ \hat{s}=c_1' \hat{e}_1+c_2' \hat{e}_2+\hat{e}_3,\end{cases} \tag{13}$$

where s is the sliding mode surface; $\boldsymbol{e}=[e_1 \quad e_2 \quad e_3]^{\mathrm{T}}$ is the tracking error of the track state, and $e_1=x_{\mathrm{d}}-x_1$, $e_2=\dot{x}_{\mathrm{d}}-x_2$, $e_3=\ddot{x}_{\mathrm{d}}-x_3$, x_{d} are the expected displacements of the piston rod of the bucket cylinder; $c_1>0$, $c_2>0$; $\hat{s}$ is the sliding mode surface of the observer, $\hat{\boldsymbol{e}}=[\hat{e}_1 \quad \hat{e}_2 \quad \hat{e}_3]^{\mathrm{T}}$, $\hat{e}_1=x_{\mathrm{d}}-z_1$, $\hat{e}_2=\dot{x}_{\mathrm{d}}-z_2$, $\hat{e}_3=\ddot{x}_{\mathrm{d}}-z_3$, $c_1'>0$, $c_2'>0$.

The differential of the sliding mode surface is

$$\dot{s}=c_1\dot{e}_1+c_2\dot{e}_2+\dot{e}_3=$$
$$c_1 e_2+c_2 e_3+\ddot{x}_{\mathrm{d}}-a_1 x_2-a_2 x_3-fu. \tag{14}$$

The SMC based on exponential reaching law is adopted, that is

$$\dot{s}=-\varepsilon\,\mathrm{sgn}(s)-ks,\ \varepsilon>0, k>0. \tag{15}$$

From Eqs. (14) and (15), the following control laws can be obtained as

$$u=\frac{1}{f}\left[c_1 e_2+c_2 e_3+\ddot{x}_{\mathrm{d}}-a_1 x_2-a_2 x_3+\varepsilon\,\mathrm{sgn}(s)+ks\right]. \tag{16}$$

The SMC control law based on the LESO can be obtained as

$$u'=\frac{1}{f}\,[c_1'\hat{e}_2+c_2'\hat{e}_3+\ddot{x}_{\mathrm{d}}-a_1 z_2-a_2 z_3-$$
$$z_4+\varepsilon\,\mathrm{sgn}(\hat{s})+k\hat{s}]. \tag{17}$$

2.3 Closed-loop stability proof

The Lyapunov function is designed as

$$V=\frac{1}{2}\hat{s}^2. \tag{18}$$

Then, we can get

$$\dot{V}=\hat{s}\dot{\hat{s}}. \tag{19}$$

According Eq. (19), there is

$$\dot{V}=\hat{s}(c_1'\hat{e}_2+c_2'\hat{e}_3+\ddot{x}_{\mathrm{d}}-a_1 z_2-a_2 z_3-z_4-fu')=$$
$$\hat{s}\Big\{c_1'\hat{e}_2+c_2'\hat{e}_3+\ddot{x}_{\mathrm{d}}-a_1 z_2-a_2 z_3-z_4-$$
$$f\Big[\frac{1}{f}(c_1'\hat{e}_2+c_2'\hat{e}_3+\ddot{x}_{\mathrm{d}}-a_1 z_2-a_2 z_3-z_4+$$
$$\varepsilon\,\mathrm{sgn}(\hat{s})+k\hat{s})\Big]\Big\}=\hat{s}(-\varepsilon\,\mathrm{sgn}(\hat{s})-k\hat{s})\leqslant 0. \tag{20}$$

According to Lyapunov stability theorem, the control system is stable.

3 Simulation

Through the co-simulation platform, the performance of the designed controller can be evaluated efficiently[8]. The complex hydraulic system was modeled in AMESim, the controller was designed in Matlab/Simulink, and the memory module was used to eliminate the algebraic loops in the system. The simulation model is shown in Fig.4.

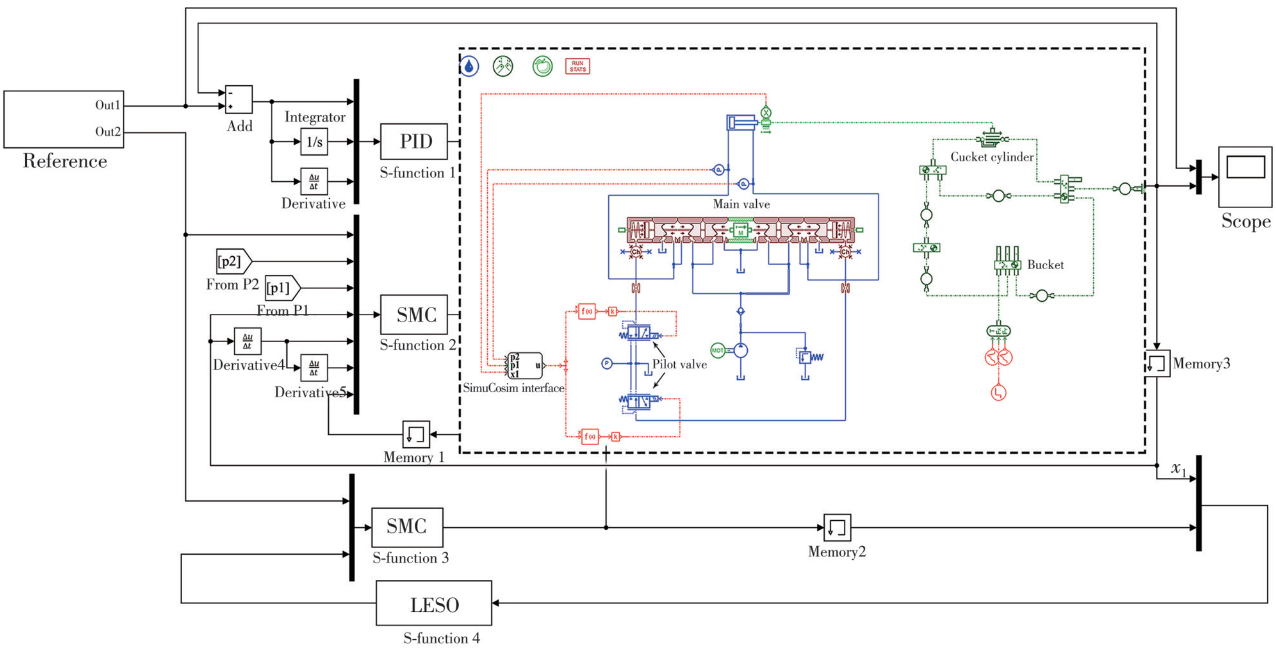

Fig. 4 Co-simulation model of bucket electro-hydraulic system

The control law was written in the S-function module, as shown in Fig.5.

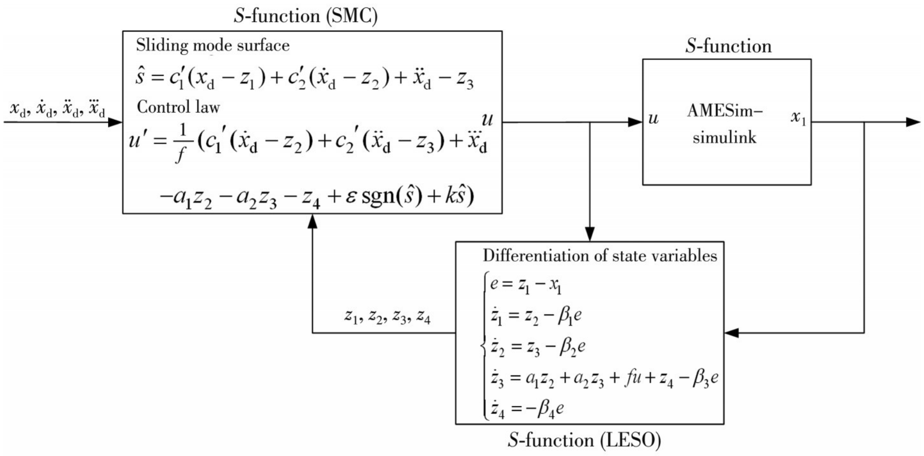

Fig. 5 Block diagram of S-Function

Hydraulic library of AMESim software was used to establish the model of electro-hydraulic proportional system, hydraulic component design (HCD) library was used to establish the model of main valve, and the working device was modeled by planar mechanical (PLM) library and the load was added at the end of bucket. The data transfer between the two softwares was achieved by the co-simulation interface. The SMC needed the input of pressure and displacement signals, while the SMC-LESO only needed the displacement signals as inputs. The output signal of the controller was used as the control signal of the electro-hydraulic proportional valve, which controlled the extension and retraction of the piston rod indirectly. The simulation time was set to be 10 s, the sampling step was set to 0.001 s, and the main parameters of the model were set as listed in Table 1.

Table 1 Parameters of co-simulation model of bucket electro-hydraulic system

Parameter	Value
Amplification coefficient/(A•V^{-1})	0.2
Control pressure at reference intensity/bar	50
Piston diameter /mm	130
Rod diameter/mm	90
Cylinder stoke/m	1
Equivalent mass of moving part/kg	400
Viscous friction coefficient/(N•s•m^{-1})	13 255
Density of fluid/(kg•m^{-3})	860
Equivalent mass of main valve spool/kg	1
Spool diameter of main valve/mm	30
Rod diameter of main valve/mm	18

To verify the effectiveness of the designed controller, its control effect was compared with that of PID controller and SMC. Step signal and sine signal were as inputs to verify the tracking performance of the controller. In addition, according to the bucket digging action, a custom continuous signal was set as an input signal for verification, as shown in Fig.6.

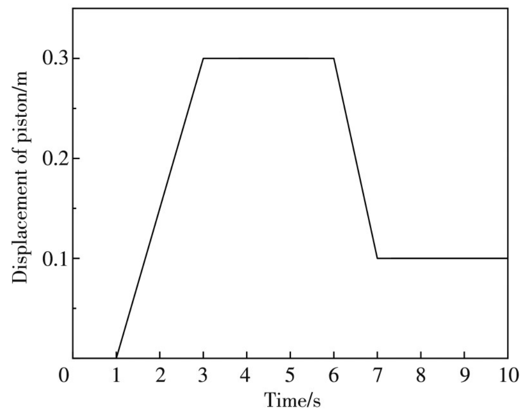

Fig. 6 Custom continuous signal

The parameter settings of the controller are shown in Table 2.

Table 2 Parameters of SMC-LESD

Parameter	Value
A_1/m^2	1.33×10^{-2}
A_2/m^2	0.69×10^{-2}
M/kg	400
V_{10}/m^3	1.33×10^{-3}
V_{20}/m^3	6.21×10^{-3}
B_c/(N•s•m^{-1})	13 255
β_e/bar	1 000
C_d	0.62
ω/mm	0.025
ρ/(kg•m^{-3})	860
p_s/bar	300
p_r/bar	0
K_1/(m•V^{-1})	0.2

Simulation were carried out under load disturbance and no-load disturbance, respectively. By comprehensively analyzing the transient response and steady-state performance of the system, the parameters of PID controller were set as $k_p=1.5$, $k_i=0.001$, $k_d=0$; the parameters of the SMC were set as $c_1 = 50\,000$, $c_2 = 10$, $\varepsilon = 10$, $k = 50$; and the parameters of SMC-LESO were set as $c_1' = 50\,000$, $c_2' = 10$, $\varepsilon = 10$, $k = 50$, $\omega_0 = 20$.

The simulation results of the step response of the three controllers without load disturbance are shown in Fig.7. It can be seen that all three controllers can achieve the accurate tracking of the specified displacement. The tracking errors of the three controllers for the step signal are shown in Fig.8. The SMC has the smallest tracking error until 3 s, the SMC-LESO reaches the steady state first, and the steady state errors of all three controllers in response to the step signal are 0.

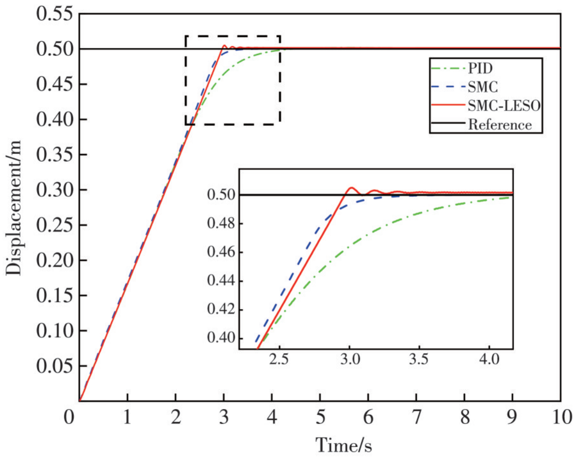

Fig. 7 Step response curves without load disturbance

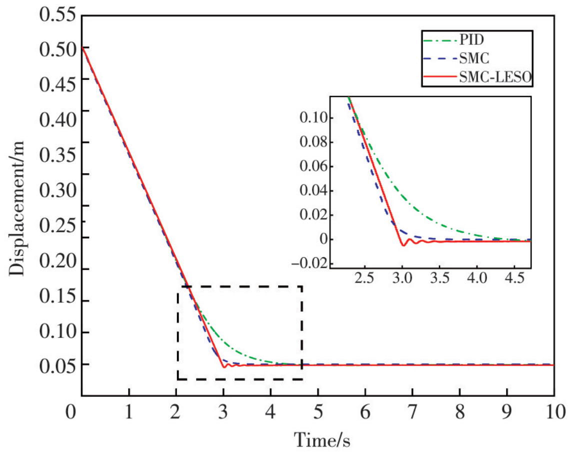

Fig. 8 Step signal tracking errors of three controllers

The response curves of the three controllers to sinusoidal signals are shown in Fig.9. The initial response speed of SMC is faster, and the SMC-LESO can realize the accurate tracking of dynamic displacement. The tracking error of sinusoidal signal is shown in Fig.10. The control error of SMC is the smallest before 2 s, and then the tracking error of SMC-LESO reaches almost 0, which is the best among the three controllers.

The tracking results of custom control signals are shown in Fig.11, and the tracking errors of three controllers are shown in Fig.12.

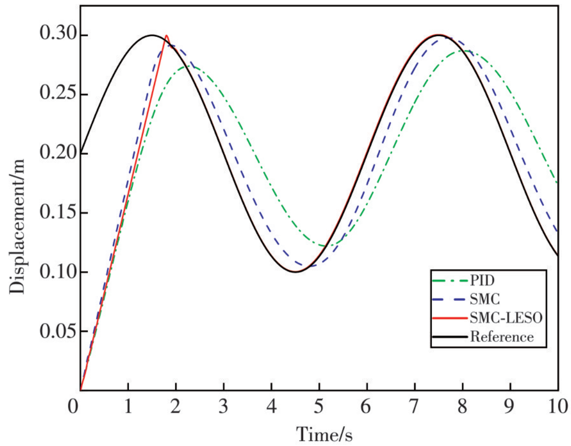

Fig. 9 Sinusoidal response curves without load disturbance

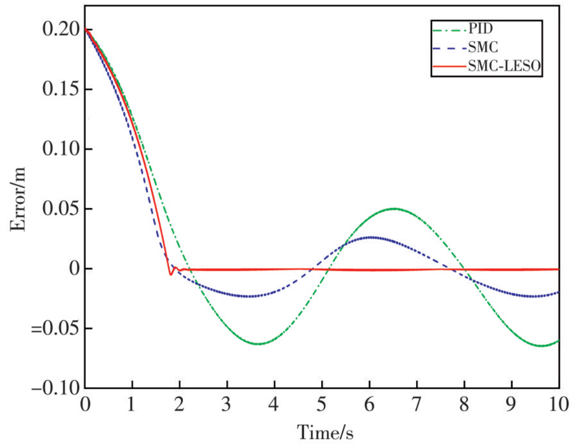

Fig. 10 Sinusoidal tracking errors without load disturbance

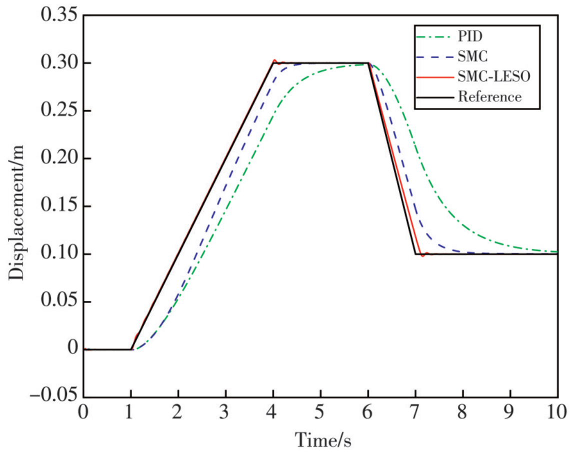

Fig. 11 Response curves of custom signal without load disturbance

It can be seen that SMC-LESO has the smallest tracking error and the best control effect compared with the other two controllers.

Excavation robots work in various ways, and the load types are complex. To simulate the performance of electro-hydraulic system of excavation robot under load disturbance, a step force of 100 kN was applied in the third second.

Under the step load disturbance, the tracking results and the tracking errors of sinusoidal signal and self-custon continuous signal are shown in Figs.13—16, respectively.

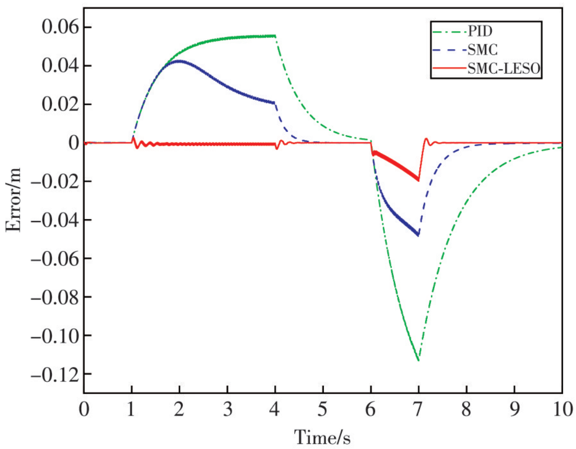

Fig. 12 Tracking errors of custom signal without load disturbance

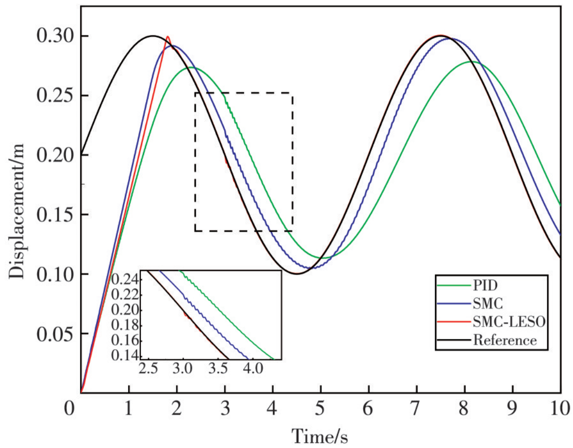

Fig. 13 Sinusoidal response curves under step load disturbance

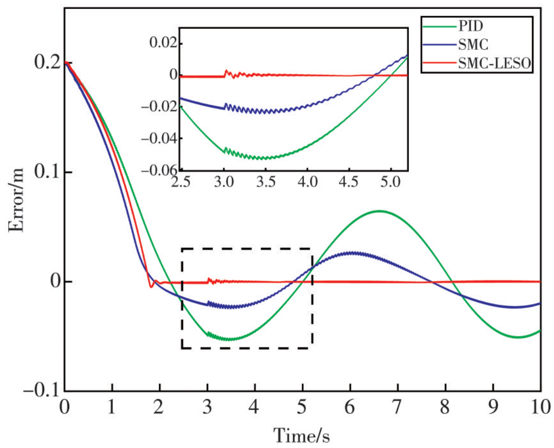

Fig. 14 Tracking errors of sinusoidal signal under step load disturbance

Comparing the control results of the three controllers, SMC-LESO has the best anti-load disturbance performance, and the system can achieve stability in the shortest time with the smallest tracking error, while SMC takes the longest time to achieve stability after fluctuation.

To better verify the performance of the controller, the load disturbance signal was set as a pulse signal, as shown in Fig.17.

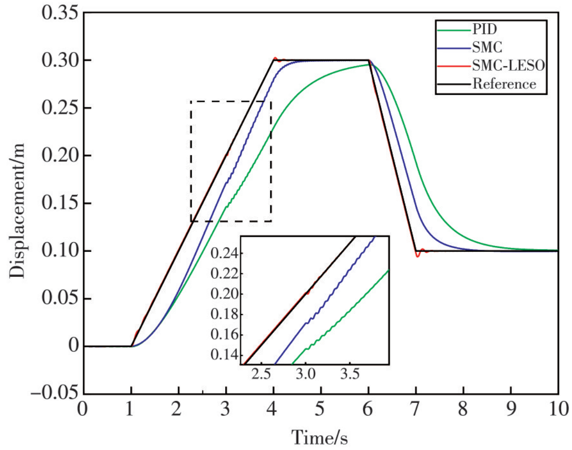

Fig. 15 Response curves of custom signal under step load disturbance

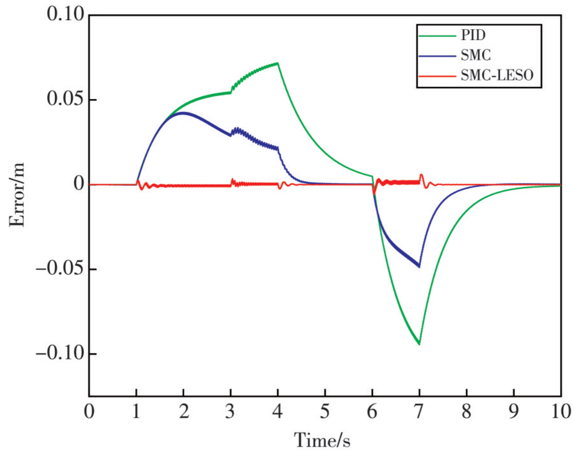

Fig. 16 Tracking errors of custom signal under step load disturbance

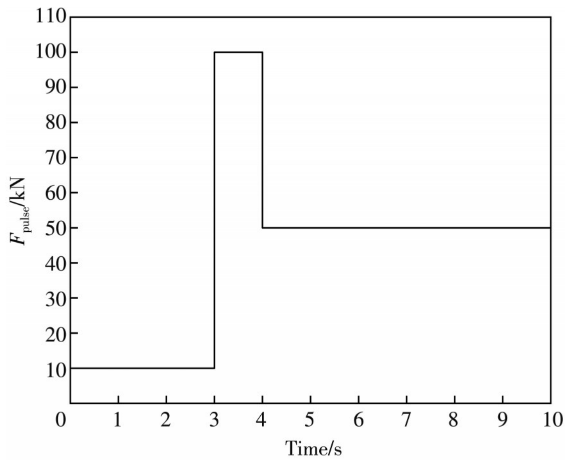

Fig. 17 Pulse load force

Under pulse disturbance, the response curves and tracking errors of sinusoidal signal and custom signal are shown in Figs.18—21, respectively.

It can be seen from Fig.18 that the initial response speed of SMC is faster, but SMC-LESO can achieve accurate tracking after 2 s. Under load disturbance, SMC-LESO is impacted minimum, SMC appears jittery, and PID controller has the worst tracking effect.

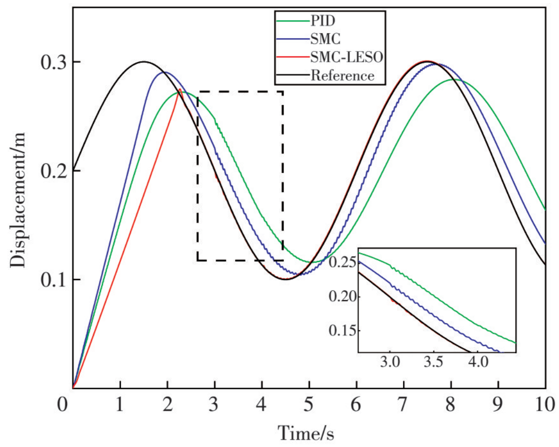

Fig. 18 Sinusoidal response curves under pulse load disturbance

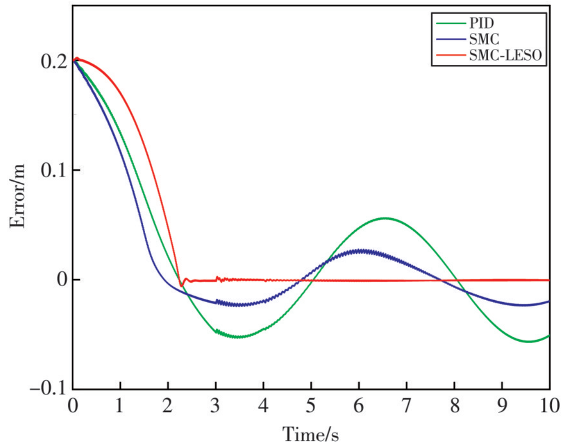

Fig. 19 Tracking errors of sinusoidal under pulse load disturbance

It can be seen that from Fig. 19 that the tracking error of SMC in the early stage is the smallest among the three controllers, but after the system is stable, the tracking error of SMC-LESO is close to 0. In Fig. 20, the anti-pulse load disturbance of SMC-LESO is the best, and the system can achieve stability in the shortest time; SMC is jittery; and PID controller has the worst tracking performance. Fig. 21 shows that SMC-LESO has the smallest tracking error under load disturbance, and is the best among the three controllers.

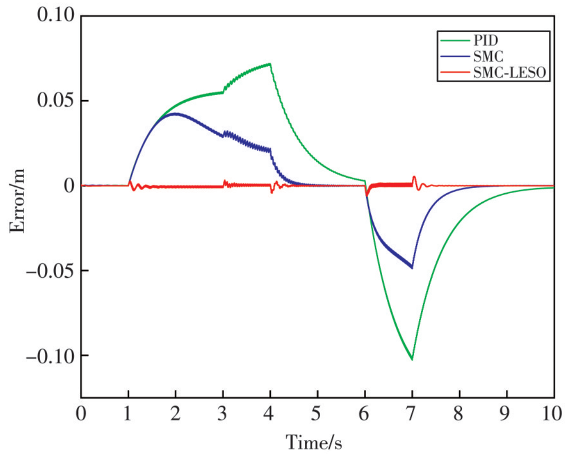

Fig. 21 Tracking errors of custom signal under pulse load disturbance

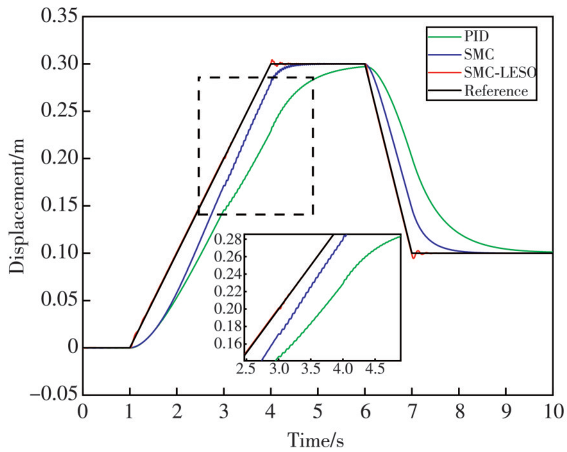

Fig. 20 Response curves of custom signal under pulse load disturbance

In order to analyze the control effects of the three controllers quantitatively. The mean absolute errors (MAE) and root mean square error (RMSE) obtained from data analysis of custom trajectory tracking error are shown in Table 3.

Table3 Comparison of performance evaluation indexes

Methods	MAE		RMSE	
	Step load disturbance	Pulse load disturbance	Step load disturbance	Pulse load disturbance
PID	3.07×10^{-2}	3.18×10^{-2}	8.7×10^{-3}	6.3×10^{-3}
SMC	1.46×10^{-2}	1.44×10^{-2}	4.9×10^{-3}	4.7×10^{-3}
SMC-LESO	$4.588\,5\times10^{-4}$	$4.168\,4\times10^{-4}$	$4.741\,5\times10^{-5}$	$7.585\,7\times10^{-5}$

MAE reflects the average level of control error. It can be seen that the MAE using our control method is improved by 98.51% and 96.86% compared with that using PID and SMC, respectively. RMSE reflects the dispersion degree of data. It can be seen that the RMSE using our control method is obviously smallest compared with that of other two control methods.

4 Conclusions

To eliminate the influence of load disturbance on trajectory control of unmanned excavation robot in the complex working environment, the SMC-LESO was adopted to analyze the system stability. Based on this, the co-simulation model of the electro-hydraulic control system was established and the simulation was carried out. Finally, the conclusions are obtained as follows.

1) SMC-LESO only needs to detect the displacement of the piston rod, which can achieve the observation of other state variables and reduce the use of sensors effectively. Compared with SMC, SMC-LESO reduces the control cost.

2) For the different forms of load on the excavation robot, we used the step signal and pulse signal to simulate the load disturbance. The simulation results show that the SMC-LESO has better anti-load disturbance performance, the smallest tracking error and the best robustness compared to PID and SMC.

Acknowledgement

This work was supported by Key Project of Industrial Science and Technology of Shaanxi Province (No.2015 GY068)

Declaration of conflicting interests

The authors have no conflict of interests related to this publication.

References

[1] ZHAO J, LONG P, WANG L, et al. AES: Autonomous excavator system for real-world and hazardous environments. 2020-11-10[2022-12-31]. DOI: 10.48550/arXiv.2011.04848.

[2] FENG H, YIN C, LI R, et al. Flexible virtual fixtures for human-excavator cooperative system. Automation in Construction, 2019, 106: 102897.

[3] YANG K S, LIU J, GU Y M, et al. On the anti-interference of electro-hydraulic control system for excavator's digging bucket arm. Journal of Northeastern University (Natural Science Edition), 2010, 31(5): 713-718.

[4] LIU G, YANG L, WU D, et al. Development and experimental investigation of an automatic control system for an excavator. Proceedings of the Institution of Mechanical Engineers, Part C: Journal of Mechanical Engineering Science, 2020, 235(4): 758-73.

[5] WANG X. Fuzzy-PID control in electro-hydraulic proportional valve system//IEEE International Conference on Computer-aided Industrial Design & Conceptual Design, November 17-19, 2010, Yiwu, China. New York: IEEE, 2020: 1454-1457.

[6] YE Y, YIN C B, GONG Y, et al. Position control of nonlinear hydraulic system using an improved PSO based PID controller. Mechanical Systems and Signal Processing, 2017, 83: 241-59.

[7] FENG H, YIN C B, WENG W W, et al. Robotic excavator trajectory control using an improved GA based PID controller. Mechanical Systems and Signal Processing, 2018, 105: 153-168.

[8] FENG H, YIN C, MA W, et al. Parameters identification and trajectory control for a hydraulic system. ISA Transactions, 2019, 92: 228-240.

[9] LI B, YAN J, GUO G, et al. High performance control of hydraulic excavator based on Fuzzy-PI soft-switch controller//IEEE International Conference on Computer Science and Automation Engineering, June 10-12, 2011, Shanghai, China. New York: IEEE, 2011: 676-679.

[10] HASSAN M Y, KOTHAPALLI G. Interval Type-2 fuzzy position control of electro-hydraulic actuated robotic excavator. International Journal of Mining Science and Technology, 2012, 22(3): 437-445.

[11] CHEN H. Research of the electro-hydraulic servo system based on rbf fuzzy neural network controller. Journal of Software, 2012, 7(9): 1960-1967.

[12] LYU G M, SUN L N, XUE Y. BP network control over the track of working device of hydraulic excavator. Chinese Journal of Mechanical Engineering, 2005, 41(5): 119-122.

[13] PI Y, WANG X. Trajectory tracking control of a 6-DOF hydraulic parallel robot manipulator with uncertain load disturbances. Control Engineering Practice, 2011, 19(2): 185-193.

[14] XU J, YOON H S. Sliding mode control of hydraulic excavator for automated grading operation. SAE International Journal of Commercial Vehicles, 2018, 11(2): 1.

[15] XU Y, LIU K. Sliding mode impedance control for the excavator's electrohydraulic system. Machine Tool & Hydraulics, 2015, 43(22): 138-141.

[16] LIU K. Research on electro-hydraulic control technology of robotic excavator's working device. Xi'an: Northeastern University, 2009.

[17] WANG H J. Research on an adaptive sliding mode control strategy for electro-hydraulic position servo system. Shanghai: Shanghai Jiao Tong University, 2017.

[18] BAI Y, PING L. Adaptive fuzzy sliding mode control for Electro-hydraulic position servo system//IEEE 2010 Chinese Control and Decision Conference, May 26-28, Xuzhou, China. New York: IEEE, 2010. DOI: 10.1109/CCDC.2010.5498613

[19] ZHU N. Electro-hydraulic position active disturbance rejection control of asymmetric valve-controlled cylinder. Electrokinetic Tool, 2020(1): 19-23.

[20] LI Y. Study on bucket trajectory and swing torque control for the autonomous hydraulic excavator. Hangzhou: Zhejiang University, 2018.

[21] YAO W L, QI G H, CHI R H, et al. Model-free adaptive control for water well drilling rig electro-hydraulic servo with unknown load disturbance. Control Theory & Applications, 2022, 39(2): 231-240.

[22] HAN J Q. Active disturbance rejection control technique – the technique for estimating and compensating the uncertainties. Beijing: National Defense Industry Press,

2008.
[23] HAN J Q. From PID technique to active disturbances rejection control technique. Control Engineering of China, 2002(3):13-18.
[24] YANG W Q, LU J H, JIANG X, et al. Design of quadrotor attitude active disturbance rejection controller based on improved ESO. Systems Engineering and Electronics, 2021, 32:1-9.
[25] WANG L X, ZHAO D X, LIU F C, et al. Linear active disturbance rejection control for a class of electro-hydraulic position servo system with light load. Control Theory & Applications, 2021, 38(4): 503-515.
[26] YU B, LI X B, YAO J, et al. Study on active disturbance rejection control of electro hydraulic servo system for 60 MN hydraulic press. Forging & Stamping Technology, 2015, 40(9): 74-79.
[27] GAO Z. Scaling and bandwidth-parameterization based controller tuning//The American Control Conference, June 4-6, 2003, Denver, Cororado. New YORK: IEEE, 2003: 4989-4995.
[28] HUANG J Z, CEN Y W, YE X H, et al. Variable load sliding mode control for manipulator based on linear extended state observers. Machine Tool & Hydraulics, 2021, 49(13): 45-50.

基于线性扩张状态观测器的挖掘机电液系统滑模控制

张　森，张　平*，赵　哲

西安建筑科技大学 机电工程学院，陕西 西安 710055

摘 要： 无人驾驶挖掘机器人实际工作环境恶劣，为提高铲斗在负载扰动下的轨迹跟踪精度，建立了挖掘机电液系统非线性数学模型，设计了基于线性扩张状态观测器的滑模控制器(Sliding mode controller based on linear extended state observer, SMC-LESO)。根据铲斗油缸活塞杆位移信号，利用设计的线性扩张状态观测器对系统的速度、加速度及负载扰动和不确定因素进行估计，解决了系统参数难以测量的问题。在此基础上，设计了滑模控制器，并证明了该控制器的Lyapunov稳定性。为进一步验证该控制器的有效性，建立了挖掘机电液比例控制系统的联合仿真模型，并与PID控制器、滑模控制器的轨迹跟踪精度进行对比。仿真结果表明，该控制器可以有效抑制扰动，位移跟踪精度高、鲁棒性强。

关键词： 无人挖掘机器人；电液系统；线性扩张状态观测器；滑模控制；位移跟踪控制

引用格式： ZHANG Sen, ZHANG Ping, ZHAO Zhe. Sliding mode control of excavator electro-hydraulic system based on linear extended state observer. Journal of Measurement Science and Instrumentation, 2024, 15(1): 72-82.